

Case study of surface micro-waves in ultra-precision raster fly cutting

Guoqing Zhang^{a,b}, Suet To^{b,c*}, Shaojian Zhang^b, Zhiwei Zhu^b

^aCollege of Mechatronics and Control Engineering, Shenzhen University, Shenzhen 518060, PR China

^bState Key Laboratory of Ultra-precision Machining Technology, Department of Industrial and Systems Engineering, The Hong Kong Polytechnic University, Kowloon, Hong Kong, PR China

^cShenzhen Research Institute of The Hong Kong Polytechnic University, Shenzhen, PR China

* Corresponding Author / E-mail: sandy.to@polyu.edu.hk, Tel: +852-2766-6587, Fax: +852-2764-7657

Abstract: In ultra-precision raster fly cutting (UPRFC), very high frequency microwaves in the range of 3.42 MHz~6.36 MHz are found on the machined surface. This study conducted a series of theoretical and experimental investigations to discover the origin of these microwaves and how they might be suppressed. Research results show that: (i) microwaves on the machined surface are caused by the material sliding during the chip formation in UPRFC; (ii) owing to the inconsistent thickness of chips along their length direction, the microwaves accumulate at the surface-exit in each feed length; and (iii) chip thickness and tool wear change the length and distribution of the microwaves. This research provides a deep insight into the formation of microwaves along with suggestion on how to suppress them.

Keywords: microwaves; surface; tool wear; ultra-precision raster fly cutting

1. Introduction

The study of vibrations in the cutting process and their effects on the surface finish are important topics in the field of ultra-precision machining (UPM). A good understanding of the effects of vibrations on surface finish is the key to improving the quality of machined surfaces. During the UPM process there are multiple sources of vibration, including spindle vibration [1], tool tip vibration [2], self-excited vibration [3], background vibration [4] and material induced vibration [5], all of which have different effects on the surface finish. Tool-tip vibration with high natural frequencies influence surface topography at a nanometric level [6], and usually result in periodic fluctuation of the surface profile in a particular spatial frequency [7] and non-uniform zebra-stripe-like patterns on the machined surface [8]. Spindle vibration is another key factor that has a major influence on surface topography in UPM. For example, in ultra-precision diamond turning, axial vibration produces concave, periodic concentric, spiral and two-fold patterns on the machined surface [9]; and in ultra-precision raster fly cutting (UPRFC), coupled tilting vibration has a principle impact on surface topography by forming ribbon-stripe and irregular patterns on the machined surface [10]. Moreover, material property (e.g. material anisotropy) causes a variation of the cutting force, shear angle, and surface roughness, which results in periodical patterns on the machined surface [11-12].

Material sliding during chip formation is another source of vibration that affects the machined surface finish. Material sliding is a cyclic behavior in the chip formation process, which is related to the accumulation and release of cutting energy. However, very few studies have focused on material sliding behavior in chip formation and the related surface topography changes. The most comprehensive research into the relation between saw-tooth caused by material sliding and surface waves was conducted by Su et al. (2015) [13]. In their study, the correlations between

chip morphology and machined surface micro-topography at different chip serration stages encountered in high-speed cutting were explored. They found that chip serration causes microwaves on machined surfaces, which increases machined surface roughness. In addition, Du and Fei conducted a series of studies on surface topography classification and measurement in conventional milling [14-17]. However, there has been no relevant research involving UPRFC.

UPRFC is a typical intermittent cutting process, whereby the diamond tool rotates with high speed, cutting into and out of the workpiece surface intermittently, as is illustrated in Fig.1. In every rotary cut, a crater is formed while the piece and pieces of crater cutting generate the desired surface structures. UPRFC has been widely used in the fabrication of non-rotational symmetric surface structures such as V-groove, pyramid structures, F-theta lens and freeform surfaces with a nanometric surface finish and submicron form accuracy.

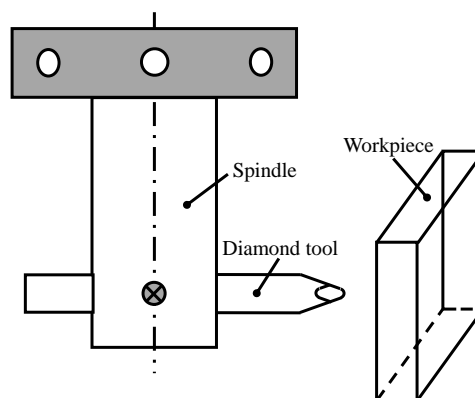


Fig. 1 Schematic of UPRFC process

Unlike high-speed cutting and single point diamond turning, UPRFC is a fly cutting process whereby the diamond tool is flying during the cutting. The intermittent cutting mechanism makes the chip morphology thinner at its two sides while thicker at its middle [18-19]. Owing to the inconsistent thickness of chips along their length direction, material sliding and its effect on the surface finish is also different. Prompted by observations of microwaves on machined surfaces, this research investigates the origin and suppressing methods of such microwaves, and provides a deep insight into the cutting mechanism and material sliding in UPRFC.

2. Experiments

In this study, the fly cutting experiments were conducted in the Precitech 705G CNC ultra-precision fly cutting machine (Precitech Inc. USA), which has five axes including three linear axes and two rotary axes. The experimental setup is shown in Fig.2. In the fly cutting process, the workpiece was mounted on a rotatable table (B axis) while the diamond tool was installed on the spindle holder that rotates circularly around the spindle axis. The commonly used CuZn30 for ultra-precision machining was used as the workpiece material, which has good diamond-machinable properties and appropriate hardness. To obtain better results, the cutting parameters used in the experiment were a little different from those commonly used. Single crystal diamond tool (Apex Inc., UK) with a rake angle of -2.5° , a clearance angle of 15° , and a tool radius of 0.631 mm was employed to cut the machined surface. The cutting parameters used in the experiment were: feed rate 200 mm/min, depth of cut 0.03 mm, spindle speed 4500 rpm, step distance 0.025 mm, swing distance 28.35 mm, a horizontal cutting strategy, and a lubricant-on cutting environment.

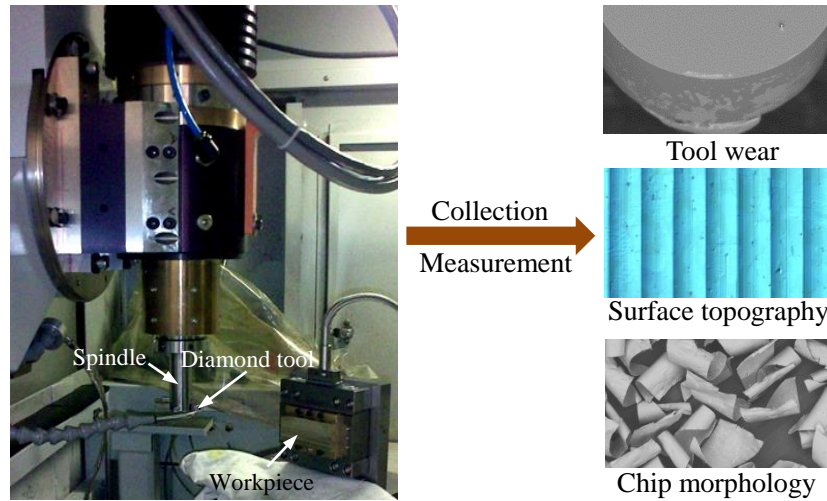


Fig.2. Experimental description

The straight cutting distance for this experiment was 5000m. Before the cutting and after each 1000m of cutting, the cutting chips were collected and examined by a Hitachi TM3000 scanning electron microscope (SEM). Simultaneously, the cutting tool and workpiece were dismantled and examined by the Hitachi TM3000 SEM and an Olympus BX60 optical microscope, respectively.

3. Results and discussion

In UPRFC, the diamond tool conducts a linear feed motion and a rotary cutting motion at the same time. Combining the two motions, the tool trajectory of the diamond tool and the machined surface topography are produced, as is shown in Fig.3 (a) and (b).

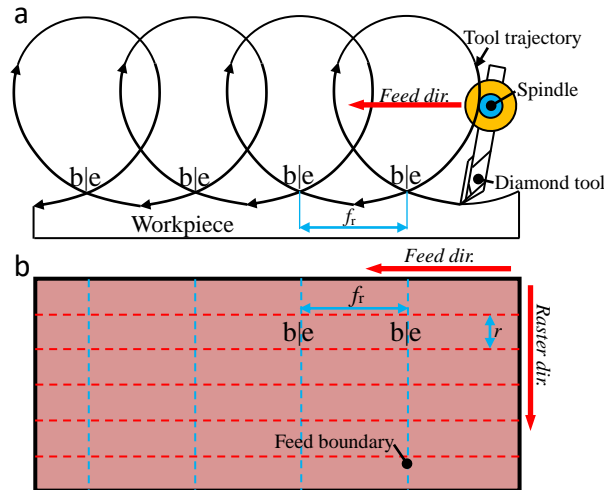


Fig.3. Schematic of cutting process in UPRFC (a) and surface generation (b)

In the experiment, a lot of microwaves were found on the machined surface with very high frequencies, as is shown in Fig.4. The length of the waves were in the range of $2.1\ \mu\text{m}$ - $3.9\ \mu\text{m}$, the microwaves accumulated into different groups with nearly the same distance between them, and the distance between two neighboring groups was about $40\ \mu\text{m}$ - $45\ \mu\text{m}$.

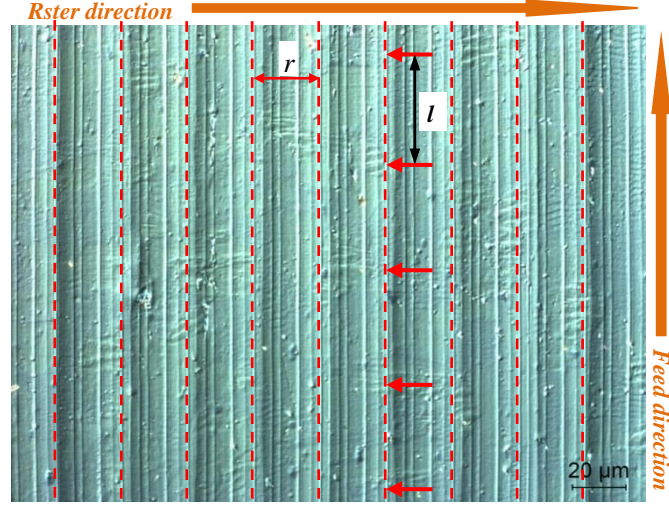


Fig.4. Microwaves appear on the machined surface

Based on the cutting parameters, the feed length in a rotary cutting can be calculated as:

$$f_r = \frac{f_e}{s_p} = \frac{200\text{mm/min}}{4500\text{r/min}} = 0.044\text{mm/r} = 44\mu\text{m/r} \quad (1)$$

Where f_r is the feed length in a rotary cutting, f_e is the feed rate in mm/min, s_p is the spindle speed.

Since the distance between two neighboring groups of microwaves is almost equal to the feed length in a rotary cutting, the microwaves on the machined surface are probably related to the rotary cutting.

According to the cutting parameters, the frequency of microwaves can be obtained. The linear velocity of the cutting tool in UPRFC can be calculated as:

$$v = \omega s_w = \frac{2\pi s_w s_p}{60} = \frac{2 \times 3.14 \times 0.02835\text{mm} \times 4500\text{rpm}}{60} = 13.35285\text{m/s} \quad (2)$$

Where ω is the angular velocity of spindle, s_w is the swing distance.

The frequency of the microwaves is calculated as:

$$\begin{cases} f_{\min} = v / w = \frac{13.35285}{3.9 \times 10^{-6}} = 3.42\text{MHz} \\ f_{\max} = v / w = \frac{13.35285}{2.1 \times 10^{-6}} = 6.36\text{MHz} \end{cases} \quad (3)$$

Where w is the length of microwaves.

Therefore, the microwaves own the frequency in the range of 3.42 MHz~6.36 MHz. This high frequency band is much higher than the frequency band of background vibration, spindle vibration, and even tool-tip vibration, and is most likely caused by material sliding during the cutting.

In continuous cutting, the cutting tool compresses a layer of workpiece material and the consequent compressive stresses cause plastic deformation by shearing, resulting in a ductile fracture of this layer. After shearing, the layer being removed becomes the chip [20]. Schematic illustrations of the continuous cutting mechanism and SEM photographs of the chip formation are show in Fig.5 (a) and (c). The uniform material sliding in continuous cutting leaves uniform microwaves on the machined surface [13]. However, UPRFC has a different cutting mechanism

whereby the intermittent rotary cutting mechanism makes the chip thickness inconsistent along its length direction in the chip formation process; that is, thinner (theoretically zero thickness) at two ends (tool entry and tool exit in Fig.5 (d)) and thicker at the middle, as is shown in Fig.5 (b) and (d). The inconsistency of chip thickness leads to non-uniform material sliding during the chip formation in UPRFC, which causes the different pitch of saw-tooth chip. Therefore, the length of microwaves on the machined surface is also different in UPRFC.

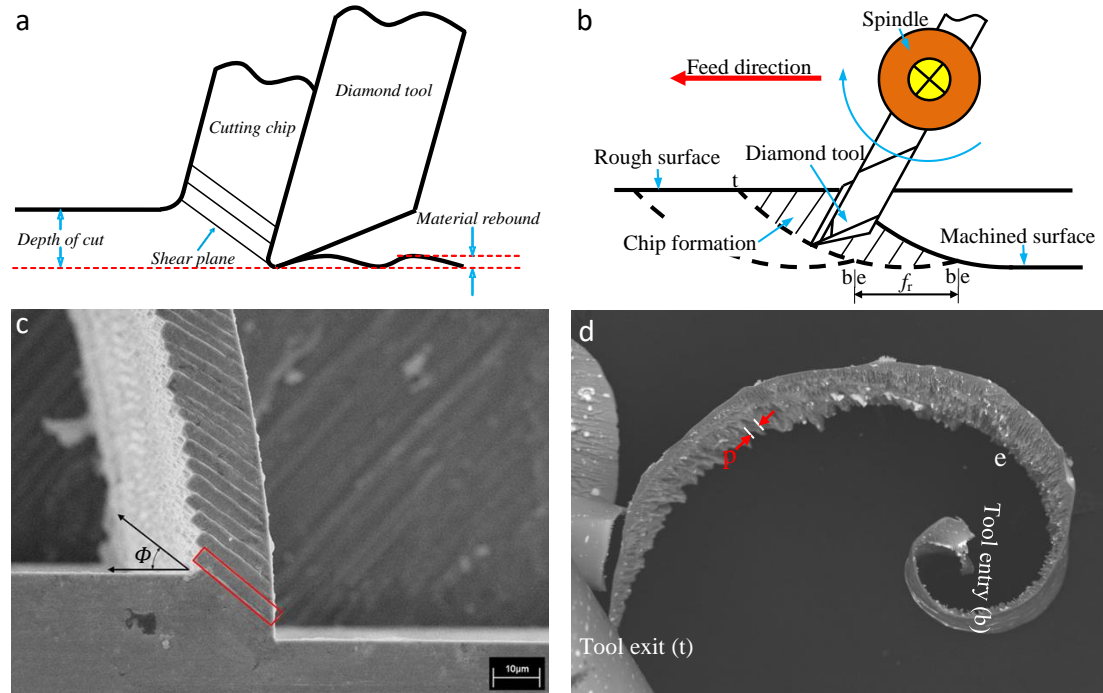


Fig.5. Schematic of continuous cutting (a) and chip formation (c)^[5], and schematic of fly cutting (b) and chip formation (d)

As not all the chip area mirrors the machined surface, only a certain area of chips can reflect the machined surface topography. As shown in Fig.5 (b) and (d), the beginning of the chip area is defined as surface-entry (point b), while the ending of the chip reflecting machined surface is named as surface-exit (point e). The distance between surface-entry and surface-exit is equal to the feed length in a rotary cutting, however it is shorter than the chip length (from point b to point t in Fig.5 (b)).

Fig.6 shows the lamella structures on the different areas of a cutting chip, owing to the thinner thickness of chips at the surface-entry and thicker thickness at the surface-exit. The pitch of lamella structure is much smaller at surface-entry of the chip (see Fig.6 (a)), while the pitch of the lamella structure is relatively large at the surface-exit of the chip. Correspondingly, the microwaves on the machined surface are exposed and accumulate at the surface-exit in each feed length due to the smaller length of microwaves at the surface-entry.

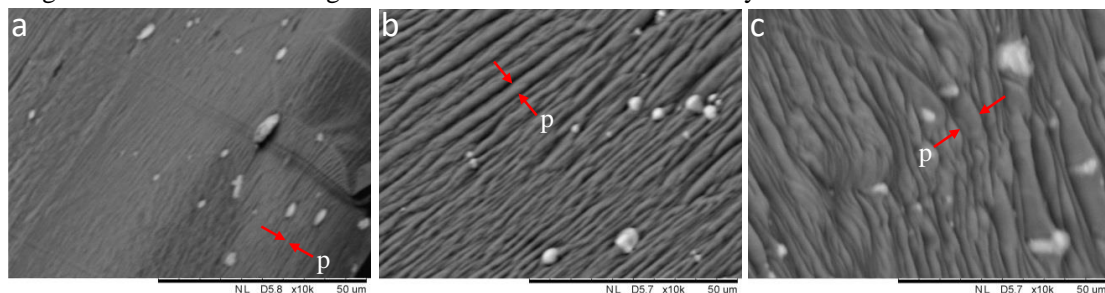


Fig.6. Lamella structure at different chip area: (a) surface-entry, (b) middle place, (c) near to surface-exit

In UPRFC, with the growing of cutting distance, tool wear features are changed correspondingly. As is shown in Fig.7, the initial tool wear features tend to be fracture on the cutting edge (e.g. F1 and F2 in Fig.7 (a)), then a wear land is formed on the cutting edge and whose width increases with the growing of cutting distance, meanwhile, the two fractures (F1 and F2) are flatten a lot, as is shown in Fig. 7 (b) and (c).

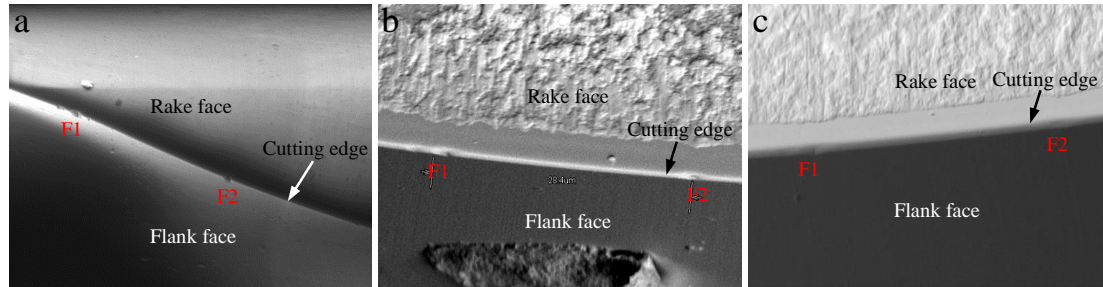

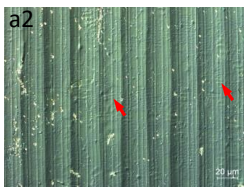
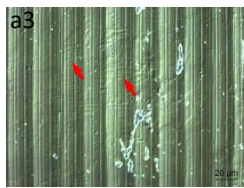
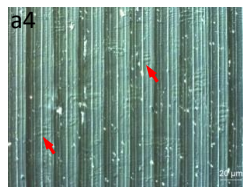
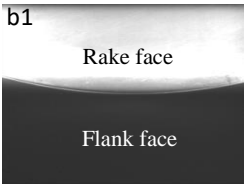
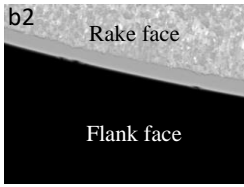
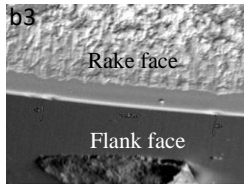
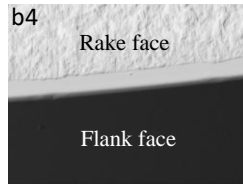
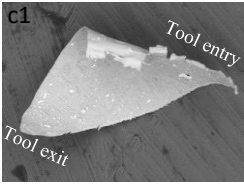
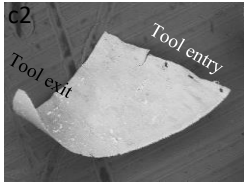
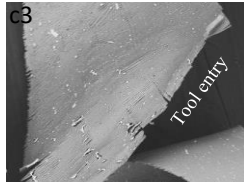
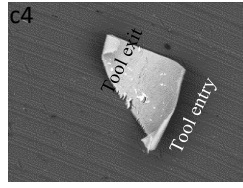


Fig.7. Tool wear features at the cutting distance of (a) 3.6m, (b) 3000m and (c) 5000m

The formation of wear land on the cutting edge affects the distribution of the microwaves. Table 1 lists the relation among tool flank wear, chip morphology and the distribution of microwaves on the machined surface. It is found that as the tool wear progresses, the tool entry of cutting chips changes correspondingly. In particular, as a wear land is formed on the cutting edge, cutting chips are truncated at both tool entry and tool exit, as is shown in Table 1 (b4) and (c4). Therefore the tool wear progress affects chip formation in UPRFC.

Table 1. Relationship among microwaves, tool wear and chip morphology

	Cutting distance:3.6m	Cutting distance:1000m	Cutting distance:3000m	Cutting distance:5000m
Micro-waves				
Tool wear				
Chip morphology				

The relation between tool flank wear and chip formation can also be reflected by the microwaves on the machined surface. It can be seen from Table 1 (a1)-(a4) that the occurrence of tool flank wear changes the distribution of the microwaves. As the tool flank wear progresses, distribution of the microwaves accumulates more at the surface-exit rather than along the whole surface of the feed length (see Table 1 (a4)); the length of the microwaves also becomes relatively large. The phenomena is thought to be related to the effect of the minimum depth of cut, at the

initial cutting stage, cutting tool with a sharp cutting edge can cut down very thin chips. However, tool flank wear increase the radius of cutting edge, therefore a ploughing instead of cutting occurs, this will lead to the accumulation of material at the surface-exit and the formation of microwaves on the machined surface.

The effects of tool wear on the length and distribution of microwaves is presented in Fig.8, which was obtained by measuring 50 wavelengths and 20 group lengths of microwaves at each cutting distance first, and then calculating their mean value and variance. It is found that with increasing cutting distance (tool wear progress) the average length of microwaves increases correspondingly; the variance of microwaves width also increases indicating that the unstable material is sliding under the tool wear. Moreover, with increasing cutting distance (tool wear progress), the group length of microwaves becomes shorter and the variance of group length decreases, meaning that the microwaves are increasingly concentrated.

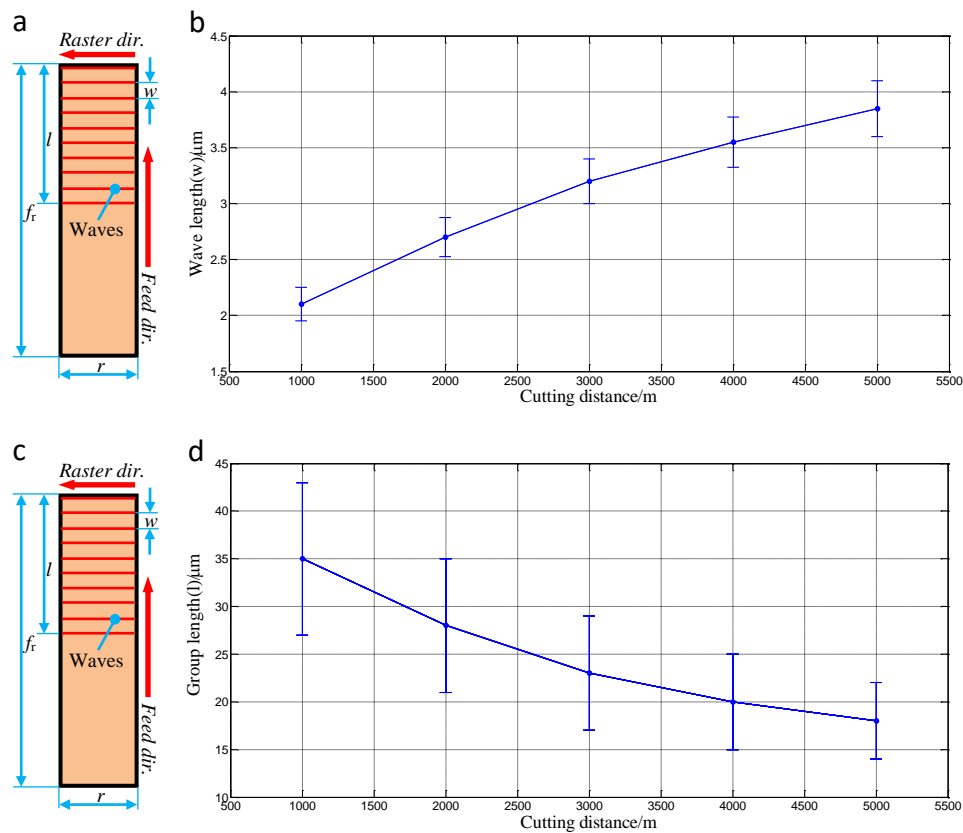


Fig.8. Relation curves of wavelength with respect to cutting distance (a-b), and group length with respect to cutting distance (c-d)

Based on the above discussion, there are two methods for suppressing microwaves on the machined surface: i) change the cutting parameters to reduce the chip thickness, and ii) suppress tool wear.

4. Conclusions

The following are the specific conclusions drawn from the foregoing research into the origin and distribution of high frequency microwaves found on UPRFC machined surfaces:

- (1) The length of microwaves on the machined surface is about 2.1μm-3.9μm, the microwaves accumulate in groups with the same distance of 40um-45um in between each group, and the microwaves own the high frequency band of 3.42 MHz~6.36 MHz.

- (2) The microwaves originate from material sliding during the chip formation due to the inconsistency of chip thickness in UPRFC, and the microwaves on the machined surface tend to accumulate at the surface-exit in each feed length.
- (3) As tool wear progresses, the length of microwaves increases while the length of each group of microwaves decreases to become more concentrated.
- (4) Reducing chip thickness and suppressing tool wear can suppress the occurrence of microwaves on the machined surface.

Acknowledgements

This project were supported by the National Natural Science Foundation of China (Grant No. 51505297 and 51275434) and Natural Science Foundation of SZU (Grant No. 836-00008418).

References

- [1]. S.J. Zhang, S. To, C.F. Cheung, H.T. Wang, Dynamic characteristics of an aerostatic bearing spindle and its influence on surface topography in ultra-precision diamond turning, *Int. J. Mach. Tools Manuf.* 62 (2012) 1–12.
- [2]. D.S. Kim, I.C. Chang, S.W. Kim, Microscopic topographical analysis of tool vibration effects on diamond turned optical surfaces, *Precision Engineering.* 26(2) (2002) 168-174.
- [3]. N. Suzuki, Y. Kurata, T. Kato, R. Hino, E. Shamoto, Identification of transfer function by inverse analysis of self-excited chatter vibration in milling operations, *Precision Engineering.* 36(4) (2012) 568-575.
- [4]. D. Lv, H. Wang, Y. Tang, Y. Huang, Z. Li, Influences of vibration on surface formation in rotary ultrasonic machining of glass BK7, *Precision Engineering.* 37(4) (2013) 839-848.
- [5]. W. Lee, S. To, C.F. Cheung, Effect of crystallographic orientation in diamond turning of copper single crystals, *Scr. Mater.* 42 (2000) 937–945.
- [6]. S.J. Zhang, S. To, G.Q. Zhang, Z.W. Zhu, A review of machine-tool vibration and its influence upon surface generation in ultra-precision machining, *Int. J. Mach. Tools Manuf.* 91 (2015) 34–42.
- [7]. H. Wang, S. To, C.Y. Chan, C.F. Cheung, W.B. Lee, A study of regularly spaced shear bands and morphology of serrated chip formation in micro-cutting process, *Scripta Materialia* 63 (2010) 227–230.
- [8]. S.J. Zhang, S. To, A theoretical and experimental investigation into multimode tool vibration with surface generation in ultra-precision diamond turning, *Int. J. Mach. Tools Manuf.* 72 (2013) 32-36.
- [9]. S.J. Zhang, S. To, H.T. Wang, A theoretical and experimental investigation into five-DOF dynamic characteristics of an aerostatic bearing spindle in ultra-precision diamond turning, *Int. J. Mach. Tools Manuf.* 71 (2013) 1–10.
- [10]. S.J. Zhang, S. To, A theoretical and experimental study of surface generation under spindle vibration in ultra-precision raster milling, *Int. J. Mach. Tools Manuf.* 75 (2013) 36–45.
- [11]. C.F. Cheung, S. To, W.B. Lee, Anisotropy of surface roughness in diamond turning of brittle single crystals, *Mater. Manuf. Process.* 17 (2) (2002) 251–267.
- [12]. W.B. Lee, C.F. Cheung, A dynamic surface topography model for the prediction of nano-surface generation in ultra-precision machining, *Int. J. Mech. Sci.* 43 (2001) 961–991.

- [13]. G. Su, Z. Liu, L. Li, B. Wang, Influences of chip serration on micro-topography of machined surface in high-speed cutting, *Int. J. Mach. Tools Manuf.* 89 (2015) 202-207.
- [14]. S. Du, L. Fei, Co-Kriging method for form error estimation incorporating condition variable measurements, *ASME Transaction on Journal of Manufacturing Science and Engineering.* 138 (2016) 041003-1-16.
- [15]. S. Du, C. Liu, L. Xi, A selective multiclass support vector machine ensemble classifier for engineering surface classification using high definition metrology, *ASME Transaction on Journal of Manufacturing Science and Engineering.* 137 (2015) 011003-1-15.
- [16]. S. Du, D. Huang, H. Wang, An adaptive support vector machine-based workpiece surface classification system using high definition metrology, *IEEE Transaction on Instrumentation and Measurement.* 64 (10) (2015) 2590-2604.
- [17]. S. Du, C. Liu, D. Huang, A Shearlet-Based Separation Method of 3D Engineering Surface Using High Definition Metrology, *Precision Engineering.* 40 (2015) 55-73.
- [18]. G. Zhang, S. To, G. Xiao, Novel tool wear monitoring method in ultra-precision raster milling using cutting chips, *Precision Engineering* 38 (3) (2014) 555-560.
- [19]. G. Zhang, S. To, G. Xiao, The relation between chip morphology and tool wear in ultra-precision raster milling, *Int. J. Mach. Tools Manuf.* 80–81 (2014) 11-17.
- [20]. V.P. Astakhov, *Tribology of metal cutting.* 52 (2006) Elsevier.